Kobe University Repository : Kernel

PDF issue: 2026-11-26

Visualization and void fraction measurement of gas-liquid two-phase flow in plate heat exchanger

Asano, Hitoshi
Takenaka, Nobuyuki
Fujii, Terushige
Maeda, N

(Citation)
Applied Radiation and Isotopes,61(4):707-713

(Issue Date)
2004-10

(Resource Type)
journal article

(Version)
Accepted Manuscript

(URL)
https://hdl.handle.net/20.500.14094/90000264

Visualization and Void Fraction Measurement of Gas-Liquid Two-Phase Flow in Plate Heat Exchanger

Hitoshi ASANO, Nobuyuki TAKENAKA, Terushige FUJII and Norio MAEDA

Department of Mechanical Engineering, Kobe University
1-1, Rokkodai-cho, Nada-ku, Kobe, 657-8501 Japan

ABSTRACT

Adiabatic and boiling two-phase flows in a simulated plate heat exchanger consisting of single passage with ribs manufactured with an angle to the flow direction were visualized by a thermal neutron radiography method. In the experiments under adiabatic condition, the air-water two-phase flows in an aluminum test section were visualized. In the boiling two-phase flow experiments, chlorofluorocarbon R141b was used as the working fluid. The two-dimensional distributions of void fraction were measured from the visualized images via some image processing techniques. As a result, it was shown that the liquid phase tended to flow straight and mixing of gas and liquid phases was a little. Moreover, in the case that a gas-liquid two-phase mixture is flowing into the test section, the phase distributions were strongly affected by the inlet configuration of the test section.

Keywords: Plate heat exchanger, Adiabatic two-phase flow, Boiling two-phase flow, Flow pattern, Void fraction, Neutron radiography

1. Introduction

A plate heat exchanger is often used in air-conditioning and refrigerating machine for the compactness and the improvement of heat transfer coefficient. Figure 1 shows a configuration of commercially-available plate heat exchanger. A plate heat exchanger is made by brazing 20～280 sheets of SUS wavy plates. Working fluids flows through the gaps between plates. The conduit of each fluid is arrayed alternately, that is, a plate heat exchanger has many parallel channels. In the case that the working fluid flows in a plate heat exchanger as gas-liquid two-phase mixture, the dynamic behaviors of gas-liquid two-phase flow greatly affect on the heat transfer performance. It is important for the design to make clear the phase distribution not only into parallel channels but also in each channel. In particular, in the case that the inlet flow is a two-phase flow, the flow pattern at the inlet of heat exchanger will affect on the phase distribution.

To make clear the behavior of two-phase flow in a complicated vessel like as a plate heat exchanger, flow visualization is efficient. However, since heat exchangers are usually made by metallic material, it is difficult to visualize by optical ray. Radiography is the visualization technique by which the structure of the object is visualized by the difference of the attenuation rate of the radio ray to the materials of the tested object. X-ray, γ-ray, and thermal and fast neutron rays are used as the radio ray in this method. The attenuation rate of thermal neutron is quite different from those of X-ray and γ -ray. Especially, the attenuation rate of thermal neutron ray is high for hydrogen contained in most working fluid, and is low for metallic element, such as aluminum, copper, and iron. Therefore, neutron radiography is very useful for the visualization of gas-liquid two-phase flow in a metallic vessel.

This study deals with the phase distribution of gas-liquid two-phase flow in a simulated plate heat exchanger with single cannel. Dynamic flow behaviors were visualized by a thermal neutron radiography method and the two-dimensional void fraction distributions were obtained via some image processing methods. From the measured results, the effect of the inlet flow pattern on void fraction distribution was considered.

2. Experimental apparatus and methods

Flow visualization experiments were carried out by utilizing JRR-3M thermal neutron radiography facility at Japan Atomic Energy Research Institute. A SIT-tube camera was used for visualization of dynamic behaviors. Continuous image of 30 frames per second were photographed. On the other hand, to measure the void fraction distribution with a high resolution, a cooled CCD camera was used. High-resolution still images consisting of 1000 x 1018 image elements were photographed with an exposure time of 4 second, and were digitized with 14 bit intensity levels. The size of visual field in the present visualization was 180 mm × 180 mm, so the spatial resolution of the void fraction distribution obtained by using the system was estimated about 180 μm as the size of visual field per image element.

2.1 Adiabatic two-phase flow experiments

A schematic diagram of the experimental apparatus for air-water two-phase flow is shown in Fig. 2 (a). Water and air were used as the working fluids. Air was fed to a mixing section ***4*** from an air compressor through a pressure regulating valve ***3*** and a gas flow meter. Water in a tank ***1***, was fed by a pump ***2*** to the mixing section ***3*** through a water flow meter. The two-phase flow formed in the mixing section flew into the lower part of plate heat exchanger placed vertically in the irradiation room. An aluminum simulated plate heat exchanger was used as the test section. The configuration of the test section is also shown in Fig.2 (a). The test section consists of the two aluminum plates those are a front plate and a back plate, with ribs of 8 mm in width and of 2.5 mm in height. The patterns of ribs on the two plates are upside-down, i.e. V-shape and Λ-shape. A netlike conduit is shaped in the plate heat exchanger by the ribs. The hydraulic diameter of conduit is about 4.65 mm. Two-phase mixtures flew into the test section from the lower and discharged from the upper.

The experimental conditions were the liquid volumetric fluxes, j_L, of 0.02 and 0.04 m/s and the gas volumetric fluxes, j_G, of 0.35 to 8 m/s, and are plotted in Fig.3, coordinates being for j_L and j_G. Volumetric flux is defined by the following equation.

$$j_L=Q_L/A, \qquad j_G= Q_G/A \tag{1}$$

where Q is volumetric flowrate [m^3/s], and A is the total cross-sectional area of the conduit [m^2].

2.2 Boiling two-phase flow experiments

The schematic diagram of experimental apparatus for boiling two-phase flow is shown in Fig. 2(b). Hydro-chlolo-fluoro-carbon R141b ($CFCl_2$-CH_3)was used as the working fluid. R141b stored in a tank ***1*** was fed by a gear pump ***2*** to the test section through a liquid flow meter ***3*** after controlling an inlet condition by a heating section ***4***. A copper simulated plate heat exchanger was used as the test section. The configuration of the test section is also shown in Fig.2 (b). In the test section, R141b was heated by rubber heaters ***7*** put on the copper plate. Neutron beam was irradiated on the test section, and the R141b boiling two-phase flow was visualized in like manner of the air-water two-phase flow experiments. The R141b two-phase flow exhausted from the test section was condensed in a plate heat exchanger ***8***.

3. Image processing for void fraction measurement

Assuming the brightness of the image is proportional to the beam intensity on the scintillation converter and neglecting the attenuation term due to the gas phase, the brightness of two-phase flow image $S_{tp}(x,y)$, the image without liquid $S_1(x, y)$, i.e., $\alpha(x, y)=1$, and the image full of liquid $S_0(x, y)$, i.e., $\alpha(x, y)=0$, is expressed as the following equations.

$$S_{tp}(x,y) = G(x,y)\,exp[-\rho_w \mu_{mw} t_w(x,y) - \{1-\alpha(x,y)\}\rho_L \mu_{mL} t(x,y)] + O_{tp}(x,y) \quad (2)$$

$$S_1(x,y) = G(x,y)\,exp[-\rho_w \mu_{mw} t_w(x,y)] + O_1(x,y) \quad (3)$$

$$S_0(x,y) = G(x,y)\,exp[-\rho_w \mu_{mw} t_w(x,y) - \rho_L \mu_{mL} t(x,y)] + O_0(x,y) \quad (4)$$

where the subscripts of *w* and *L* mean the wall and the liquid, respectively, and *t(x, y)* means the thickness of the two-phase flow area at coordinate *(x, y)*. In this equation, α means the averaged void fraction along the neutron beam. *G(x, y)* is the gain and depends on the position due to the non-flatness of the initial beam intensity and of the sensitivity in the imaging system. *O(x, y)* is the offset. The variations of brightness caused by the neutron scattering in the object and the optical scattering in the neutron camera were evaluated as the offset value, that is, the offset is due to the dark current, the neutron scattering, and optical scattering. The offset value depends on the flow pattern. To measure the void fraction of gas-liquid two-phase flow quantitatively, it is necessary to estimate the offset value under each experimental condition.

Using Eqs. (1) to (3) , the two-dimensional void fraction distribution can be expressed as

$$\alpha(x,y) = \frac{ln[S_{tp}(x,y) - O_{tp}(x,y)] - ln[S_0(x,y) - O_0(x,y)]}{ln[S_1(x,y) - O_1(x,y)] - ln[S_0(x,y) - O_0(x,y)]} \quad (5)$$

Eq.(4) means two-dimensional void fraction distributions can be calculated without knowing the thickness and the physical properties of the wall and the liquid so far as the two images without and full of liquid and the offset for the each condition were recorded in the same configuration as the two-phase visualization.

For a visualization of dynamic behaviors of void fraction distribution, the dark current of camera system was used as the offset value, and continuous images of void fraction distribution were obtained qualitatively. On the other hand, in the quantitative measurement of void fraction distribution, the offset value *O(x, y)* was estimated by the umbra method with B_4C as neutron absorber (Takenaka, N., et al., 2001). Figure 4 shows the visualized image of water single-phase flow in the aluminum test section with the neutron absorber grid. The grid was placed between the neutron source and the object. The grid consists of the absorber rods made by B_4C powder in rectangular ducts of 3×3 mm^2. The interval of the rod is 3 mm. At the position covered with the B_4C rods, the irradiated neutron beam is absorbed in B_4C. Therefore the brightness at the back of the B_4C rods is assumed to be due to the dark current, the neutron and the optical scattering, that is, the brightness shows the offset value. As the offset value for the section without the B_4C rods, interpolated values were used.

4. Results and discussion

4.1 Adiabatic air-water two-phase flow

Figure 5 shows the original image by SIT-tube camera. Liquid flow was clearly visualized. The continuous image of calculated void fraction distributions are shown in Figs. 6 at intervals of 1/30 seconds. These figures show the qualitative distribution by Eq. (5) with a dark current image as offset value. In this figure, the void fraction distribution is shown with the brightness, that is, the void fraction of the black part is 0, and that is increasing with an increasing brightness. A gas volumetric flux j_G and a liquid volumetric flux j_L were 0.9 m/s and 0.04 m/s, respectively. Gas phase were flowing up like as large bubble in liquid phase intermittently.

Figures 7 (a) to (h) show the time averaged void fraction distribution for a constant j_L of 0.04 m/s and varied j_G of 0.9 m/s to 8.0 m/s. Flow patterns of gas-liquid two-phase flow were classified into two cases. At low volumetric flux of gas phase (j_G=0.9 m/s), gas phase intermittently flows in continuous liquid phase. On the other hand, at high volumetric flux of gas phase (j_G=8.0 m/s), the gas and liquid phases tended to flow straight upward separately. Especially, at j_G=8.0 m/s, the most of liquid phase flew along the both side and the center of the heat exchanger. The transition boundary of the flow pattern was around the j_G of 3 m/s. Under every condition, the liquid fraction at the lower part was unsymmetrical being inclined toward the left side caused by the liquid pool at the inlet of the test section. It was shown that the effect of the liquid pool remained near the exit of the test section.

The cross-sectional average void fraction distributions are plotted in Fig.8 against the distance y defined in Fig. 7. The void fraction was high at the just upstream of y=0, because the cross-sectional area became smaller at y=0 and the gas phase stagnated. In the area with ribs (y>0), though the void fractions was scattering, those seem to be stable. The fluctuations of void fraction might be due to the stagnant of liquid or gas phase at cul-de-sac on both sides of the test section.

The correlation on the averaged void fraction based upon the drift flux model is shown in Fig. 9. For the drift flux model, the relation between mean gas velocity $Q_G/(\alpha A) = j_G/\alpha$ and total volumetric flux j_G+j_L is shown by the following equation.

$$j_G/\alpha = C_0\left(j_G + j_L\right) + V_{Gj} \tag{6}$$

where C_0 is a distribution parameter which depends on the distribution of the void fraction and the volumetric flux, and V_{Gj} is the average drift velocity. The correlated results for vertical upward flow in a circular pipe by Ishii were plotted as bold lines. It can be seen in this figure that the values of C_0 and V_{Gj} for the experimental results were larger than those by Ishii's equation. It is estimated that this is caused by the unsymmetrical distribution of the liquid phase and the larger shear force on liquid phase along the left and right side.

4.2 Boiling Two-Phase Flow

The measured void fraction distributions of boiling two-phase flow are shown in Figs. 10 (a) and (b). In Fig. (a), working fluid flew into the test section as two-phase mixture with the mass vapor quality of 0.3. Fig. (b) shows the case that the inlet flow condition was a subcooled liquid with the subcooling of 17 K. In the case that the working fluid was the two-phase flow at the inlet of the test section, the liquid fraction distribution was unsymmetrical, i.e., the liquid fraction on the right side was higher than that on left side over the test section. It can be seen that the liquid pool at the inlet of test section strongly affect on the phase distribution with the same tendency as that in air-water two-phase flow. On the other hand, the tendency in Fig. (b) was different from that in Fig. (a). The black area at where the liquid fraction might be high was larger at the center. This means that the liquid flow rate must be larger. The suitable inlet configuration of heat exchanger is necessary for the each inlet condition.

5. Conclusions

To make clear the phase distribution in a plate heat exchanger, adiabatic air-water two-phase flows and R141b boiling two-phase flows in a simulated plate heat exchanger with single conduit were visualized by a neutron radiography method. Two-dimensional distributions of void fraction were measured via some image processing methods. It was shown that the flow behavior at the inlet of test section affected on the phase distribution of the void fraction.

References

Takenaka, N., Asano, H., Fujii, T., Matsubayashi, M., 2001, A Method for Quantitative Measurement by Thermal Neutron Radiography., Nondestructive Testing and Evaluation, 16, 345-354.

Ishii, M., 1977, One-Dimensional Drift-Flux Model and Constitutive Equations for Relative motion Between Phases in Various Two-Phase Flow Regimes., ANL-77-47.

List of figures

Fig.1 Configuration of commercially-available plate heat exchanger.

Fig.2 Schematic diagram of experimental apparatus and test section configuration.
(a) Air-water adiabatic two-phase flow.
(b) R141b boiling two-phase flow.

Fig.3 Experimental conditions for adiabatic air-water two-phase flow.

Fig.4 Visualized image of water single-phase flow with B_4C grid.

Fig.5 Original image by SIT-tube camera (30 fps, j_G=0.9 m/s, j_L =0.04m/s).

Fig.6 Continuous image of calculated void fraction distribution (j_G=0.9 m/s, j_L =0.04m/s).

Fig.7 (a) - (h) 2D-distributions of time-averaged void fraction calculated from the images by SIT tube camera
(j_G = 0.04 m/s).

Fig.8 One-dimensional distribution of cross-sectional averaged void fraction along the flow direction
(Quantitative measured results by umbra method from the images by cooled CCD camera).

Fig.9 Comparison of measured void fractions with those by Ishii's equation based on the drift-flux model for vertical upward flow in a circular tube.

Fig.10 Two-dimensional distribution of void fraction of boiling two-phase flow.

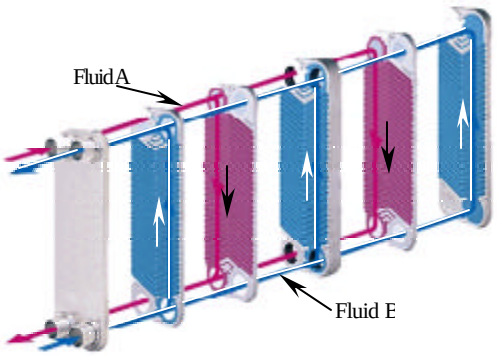

Fig. 1 Configuration of commercially-available plate heat exchanger.

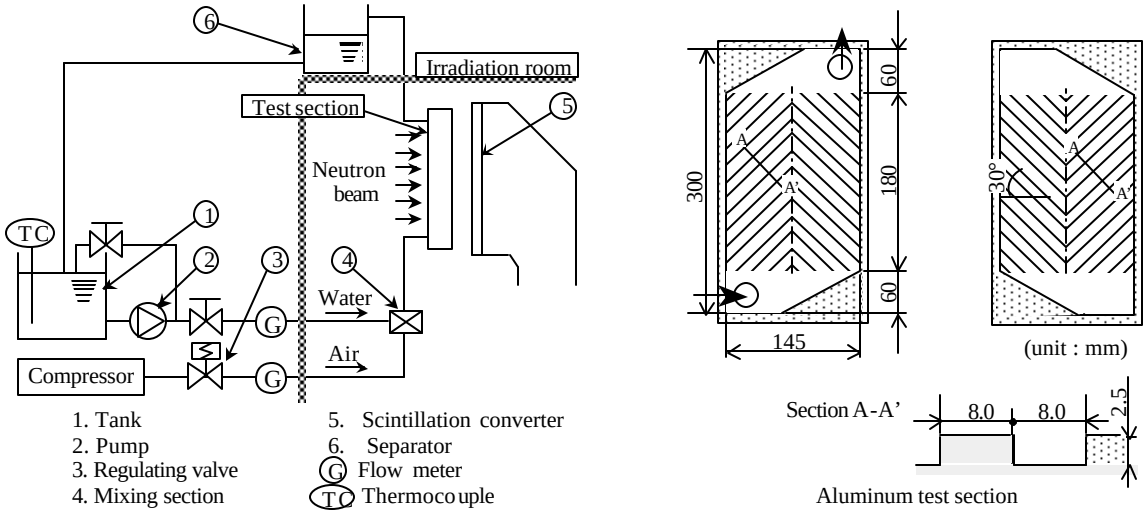

(a) Air-water adiabatic two-phase flow.

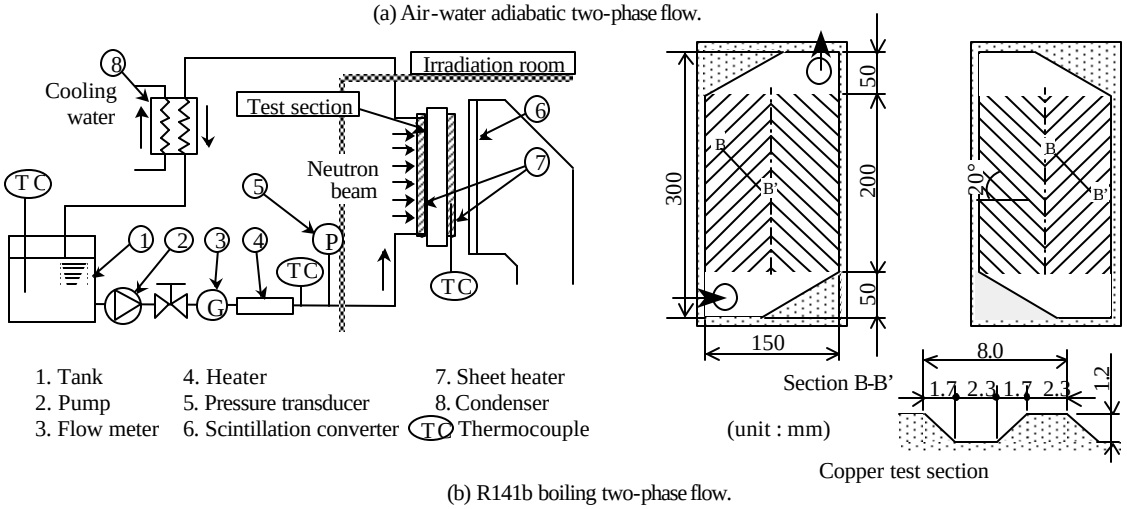

(b) R141b boiling two-phase flow.

Fig. 2 Schematic diagrams of experimental apparatus and test section configurations.

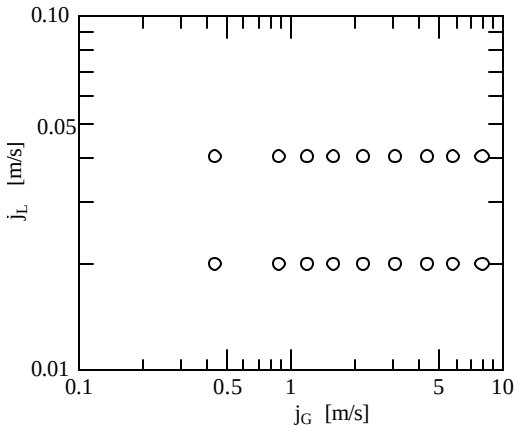

FIg. 3 Experimental conditions for adiabatic air-water two -phase flow.

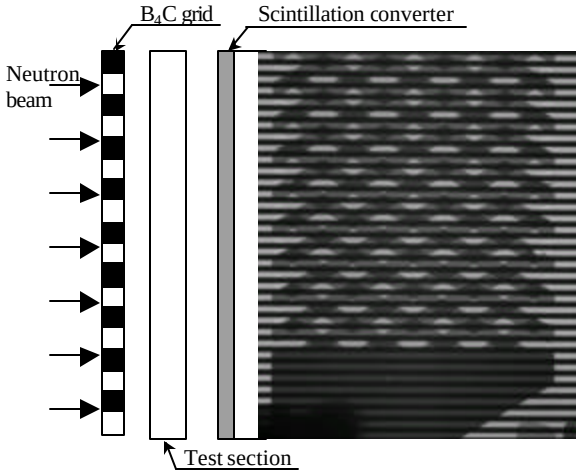

Fig. 4 Visualized image of water single-phase flow with B_4C grid.

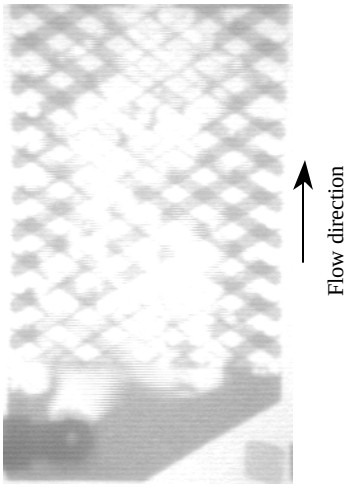

Fig. 5 Original image by SIT -tube camera.
(30 fps, j_G=0.9 m/s, j_L =0.04m/s)

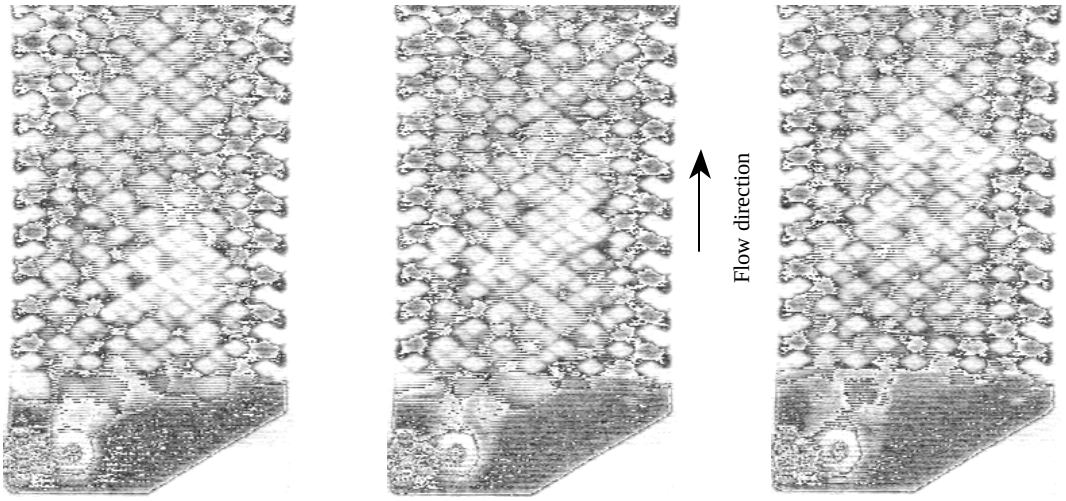

Fig. 6 Continuous image of calculated void fraction distribution (j_G=0.9 m/s, j_L =0.04m/s).

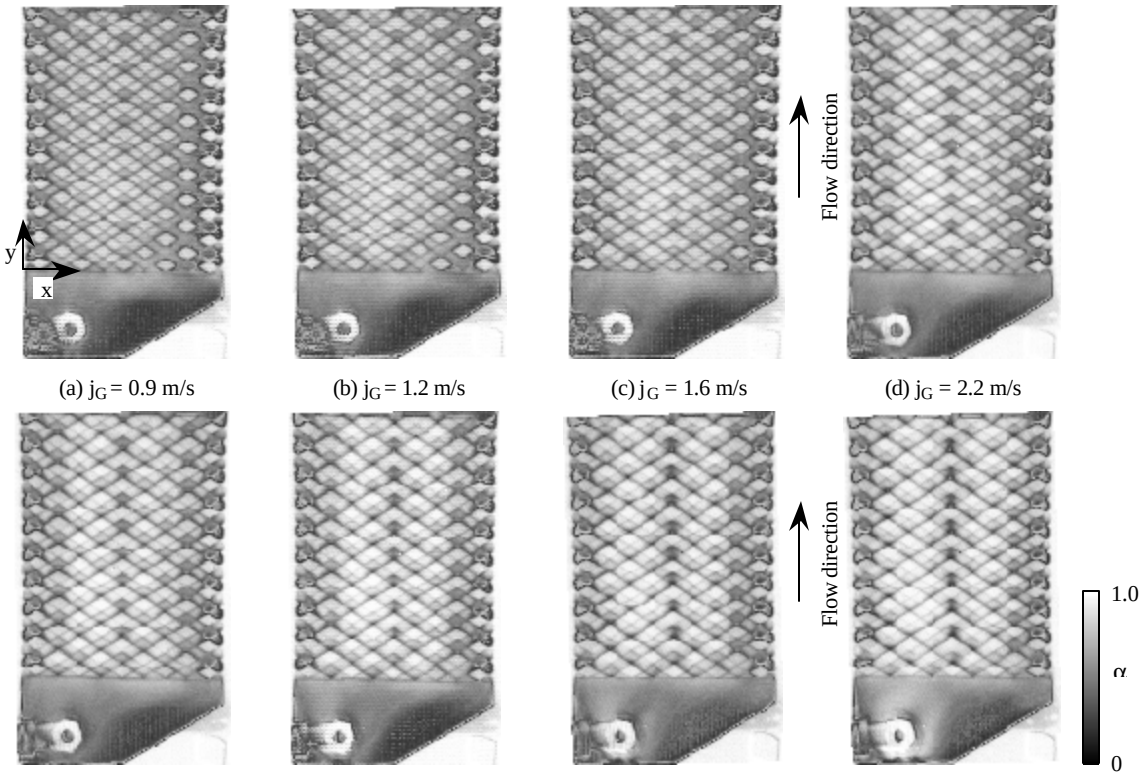

(a) j_G = 0.9 m/s (b) j_G = 1.2 m/s (c) j_G = 1.6 m/s (d) j_G = 2.2 m/s

(e) j_G = 3.1 m/s (f) j_G = 4.4 m/s (g) j_G = 5.8 m/s (h) j_G = 8.0 m/s

Fig.7 2D-distributions of time-averaged void fraction calculated from the images by SIT tube camera (j_L = 0.04 m/s).

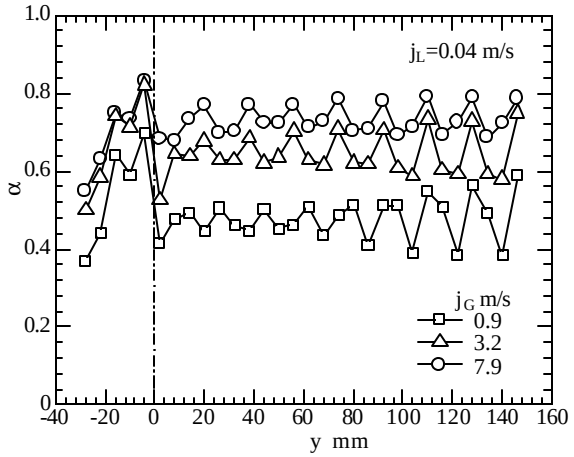

Fig. 8 One-dimensional distribution of cross-sectional averaged void fraction along the flow direction (Quantitative measured results by the umbra method from images by cooled CCD camera).

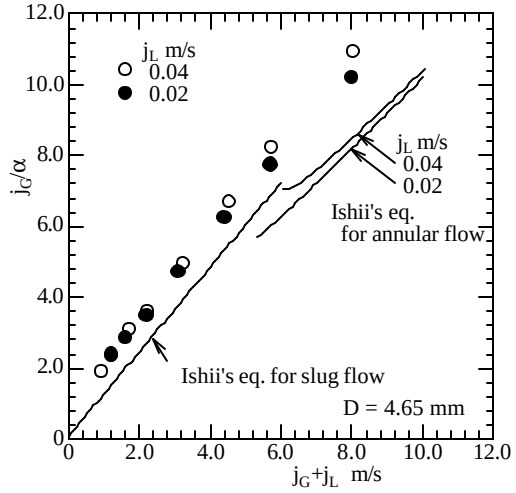

Fig. 9 Comparison of measured void fractions with those by Ishii's equation based on the drift-flux model for vertical upward flow in a circular tube.

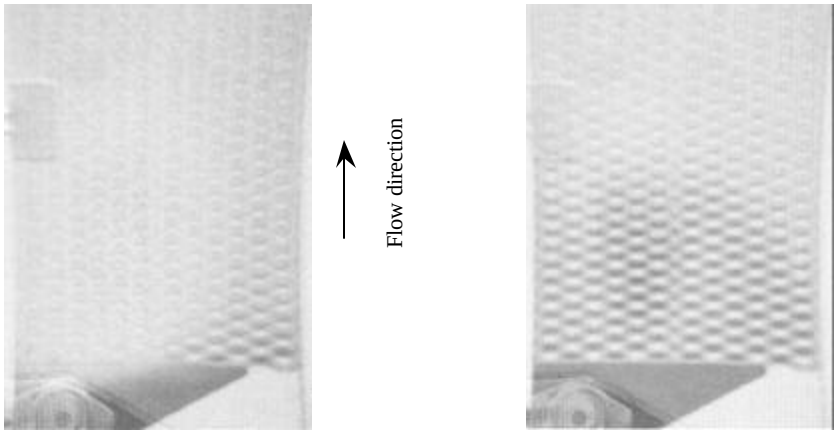

(a) Inflow of two-phase flow
(Mass flowrate: 0.0042 kg/s,
Inlet vapor mass quality: 0.3)

(b) Inflow of subcooled liquid single-phase flow
(Mass flowrate: 0.0042 kg/s,
Inlet subcooling: 17 K)

Fig. 10 Two-dimensional distribution of void fraction in boiling two-phase flow.